metals

MDPI

Article

Super Abrasive Machining of Integral Rotary Components Using Grinding Flank Tools

Haizea González [1,*], Amaia Calleja [1], Octavio Pereira [1], Naiara Ortega [1], L. Norberto López de Lacalle [2] and Michael Barton [3]

1 Department of Mechanical Engineering, University of the Basque Country (UPV/EHU), Alameda de Urquijo s/n, 48013 Bilbao, Spain; amaia.calleja@ehu.eus (A.C.); octaviomanuel.pereira@ehu.eus (O.P.); naiara.ortega@ehu.eus (N.O.)

2 CFAA—University of the Basque Country (UPV/EHU), Parque Tecnológico de Zamudio 202, 48170 Bilbao, Spain; norberto.lzlacalle@ehu.eus

3 BCAM—Basque Center for Applied Mathematics, Alameda de Mazarredo 14, 48009 Bilbao, Spain; mbarton@bcamath.org

* Correspondence: haizea.gonzalez@ehu.eus; Tel.: +34-946-017-347

Received: 28 November 2017; Accepted: 29 December 2017; Published: 1 January 2018

Abstract: Manufacturing techniques that are applied to turbomachinery components represent a challenge in the aeronautic sector. These components require high resistant super-alloys in order to satisfy the extreme working conditions they have to support during their useful life. Besides, in the particular case of Integrally Bladed Rotors (IBR), usually present complex geometries that need to be roughed and finished by milling and grinding processes, respectively. In order to improve their manufacturing processes, Super Abrasive Machining (SAM) is presented as a solution because it combines the advantages of the use of grinding tools with milling feed rates. However, this innovative technique usually needed high tool rotary speed and pure cutting oils cooling. These issues implied that SAM technique was not feasible in conventional machining centers. In this work, these matters were tackled and the possibility of using SAM in these five-axis centers with emulsion coolants was achieved. To verify this approach, Inconel 718 single blades with non-ruled surfaces were manufactured with Flank-SAM technique and conventional milling process, analyzing cutting forces, surface roughness, and dimension accuracy in both cases. The results show that SAM implies a suitable, controllable, and predictable process to improve the manufacture of aeronautical critical components, such as IBR.

Keywords: Blisk machining; super abrasive machining; SAM; Inconel 718 machining

1. Introduction

Aeronautical industry is on the path to steady growth, is one of the most strategic sectors in the worldwide economy. In fact, TEDAE association (Spatial, aeronautical, and defense technology Spanish association) states that the turnover of this industry is about 7600 million euros, from which 9.5% is aimed at R & D [1]. This economic investment stems from the need of facing global competitiveness. This is being reflected in high requirements that are related not only to mechanical properties required through all the life-cycle of these components, but also on the optimization of manufacturing process.

This is especially relevant for critical aeronautical turbomachinery components where their reliability directly affects to aeronautical jet engines security. Among them, noteworthy components are axial compressors and turbines in civil aviation. In particular, this work deals with manufacturing processes of Bladed Disks (Blisk) and Integrally Bladed Rotors (IBR). The main difference between

them is the junction of the blades to the disk. As it is shown in Figure 1, Blisk components have their blades separated from the disk, assembled through fir-trees. IBR, however, are integrated components, which are manufactured from the same blank, what avoids unions' issues [2].

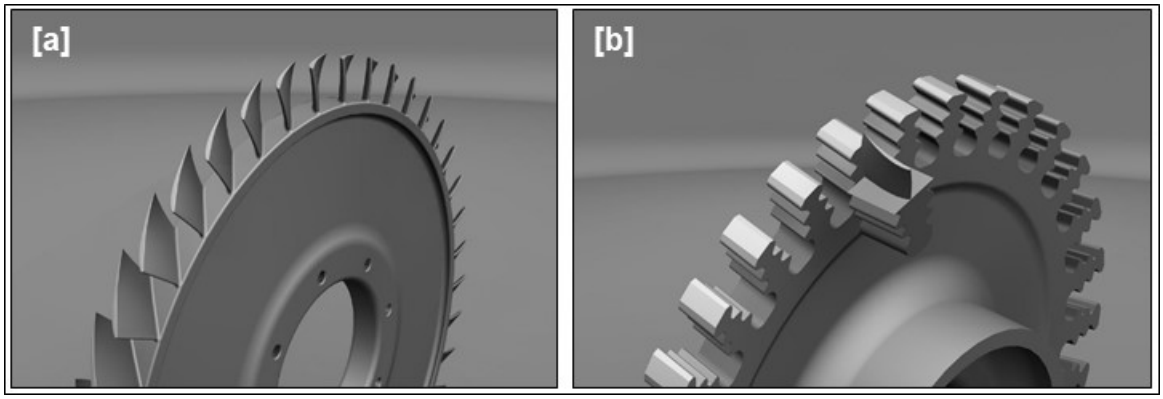

Figure 1. Compressor and turbine disk layout. (**a**) Integrally Bladed Rotor; (**b**) Blisk.

It should be noted that during its entire lifetime, these components are usually subjected to extreme working conditions, what requires high heat resistant alloys, such as titanium or nickel-based alloys. These materials are characterized for combining hardness with low thermal conduction and good ductility [3,4]. However, these alloys are known as difficult-to-cut materials, implying premature tool wear and high cutting forces [5–7]. Additionally, in the particular case of Blisk, difficulties are not only presented in blade manufacturing processes, but also as an extra challenge consists of fir-trees junctions manufacturing. This is due to the fact that these geometries are crucial for the functionality of the parts, and they possess complex geometry, together with very tight dimensional and finishing tolerances [8]. On the other hand, fir-trees have been traditionally manufactured by Electro Discharge Machining (EDM). This non-conventional manufacturing technology stands out for facilitating complex geometrical cavities of high hardness materials with dimensional accuracy and excellent finishing surface [9–11]. Notwithstanding, the main inconvenience of this technology is based on low material removal rates, what means elevated manufacturing time. For this reason, some studies look for innovative technologies to cover this deficiency. Among these technologies, Super Abrasive Machining (SAM) was presented in [12] as a solution to increase machining efficiency during the production of blades and turbine disks.

In particular, SAM is characterized by using grinding technology with machining rates. Therefore, this technology provides the precision of grinding process with similar feeds and costs to the use of single point machining. Moreover, SAM is more versatile than other grinding techniques. For example, if it is compared with creep fatigue grinding (the closest rival), the use of SAM achieves higher speeds, higher material removal rates—up to 1000 mm^3/s—with lower workpiece loads, and more accurate dimensional tolerances [12,13] is what makes this technology a suitable and efficient alternative to manufacture IBRs nickel-based super alloys [14,15]. Its application to blisk fir-trees has been realized [16,17], as it is shown in Figure 2, due to the fact that the use of this technique increases efficiency significantly.

Furthermore, SAM was tested with other more complex geometries, such as the blades from IBRs or impellers. The main advantages are higher material removal rates at high speed [18] and a near shape surface. In fact, Rolls-Royce claims, under the correct performance, that the process is capable of stock removal at a rate of 80 cubic millimeters per second per millimeter of wheel width. That is, eight times the achievable rate using plated CBN wheel technology for super abrasive machining of nickel alloys on a conventional grinding machine. The process can also achieve higher removal higher rates for fishing grinding operations than alternative methods [19]. Additionally, it is noteworthy that using these kinds of tools, due to process temperature and extreme cutting conditions, cutting fluids

are required, particularly cutting oil [20–22]. Regarding cutting conditions, in line with [23], they can be optimized with the aim of developing the exact windows parameters. Moreover, another restrictive requirement is having appropriate equipment with high speed spindles (60,000–90,000 rpm) [17], what makes this process unachievable to the most part of the current machining centers whose spindles rotary speed capacity are below 24,000 rpm.

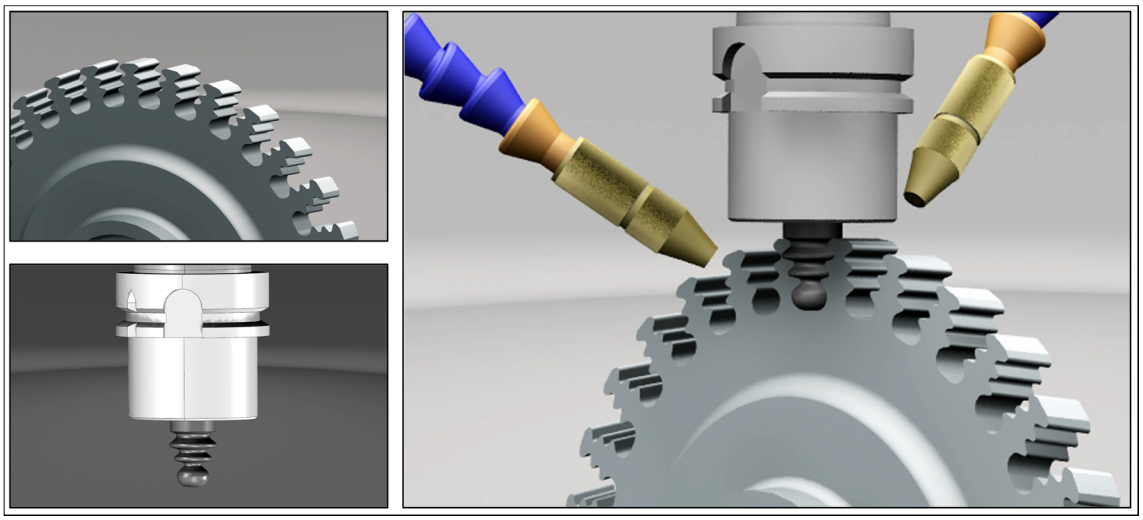

Figure 2. Super Abrasive Machining (SAM) applied for fir trees manufacturing.

In this line, the novelty of this work stems from the idea of using SAM technology instead of conventional milling technology for roughing and finishing IBR blades geometry with non-ruled surfaces, (a) using conventional machining centers with a spindle, which does not reach the high rotary speeds needed, and (b) combined with oil emulsions instead of mineral cutting oils. For this, cutting forces, surface finishing, and dimension accuracy using SAM technology were analyzed and compared with conventional milling process.

2. Experimental Setup and Tests Performance

Experimental tests were carried out in a five-axis machining center, Ibarmia ZV-25/U600 model (IBARMIA INNOVATEK, S.L.U., Guipuzkoa, Spain). This machine consists of five-axis divided into three linear axes (X, Y, Z), two rotary axes (A, C), and a spindle speed capacity of 18,000 rpm, 18 KW. Regarding machining processes, in order to compare the two different techniques (SAM and conventional milling), roughing and finishing operations with both techniques were carried out. During machining process, cutting forces were recorded with tri-axial force transducer piezoelectric dynamometer, Kistler 9255 and OROS® OR35 analyzer (OROS, Inovallee, France), with a sampling frequency of 16,384 samples per second. Figure 3 shows the experimental setup used to perform this test.

Due to aggressive conditions at which IBRs are exposed, such as high temperatures and aggressive chemical environments, they are manufactured using nickel-base superalloys [24]. In particular Inconel 718 was chosen. This material is a heat-resistant Ni-Fe alloy, which is hardened by precipitation of secondary phases into the metal matrix [25], achieving in this case an average value of hardness 42 HRC, with strain hardening affected areas on several surface points due to the initial saw cuts. The chemical composition, mechanical, and physical properties of tested materials are shown in Table 1.

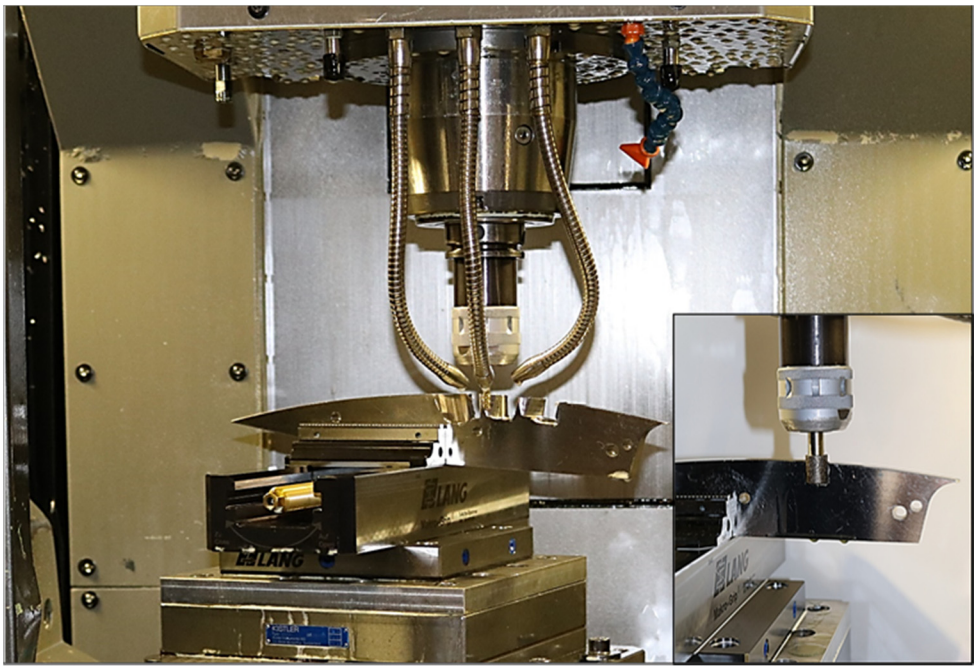

Figure 3. Experimental Setup on Ibarmia machining center, showing the IN718 circular sector.

Table 1. Inconel 718 chemical composition (%), mechanical and physical properties [26,27].

Ni	Cr	Co	Fe	Nb	Mo	Ti	Al	B	C	Mn	Si	Others
52.5	19	1	17	5	3	1	0.6	0.01	0.08	0.35	0.35	1.79
Hardness		Young's Modulus		Tensile Strength		Density		Specific Heat		Melting Temp.		Thermal Conduct
42 HRc		206 GPa		1.73 GPa		8470 kg/m^3		461 J/(kg·K)		1550 K		15 W/(m·K)

The alloy offers good resistance to fatigue and creep combined with high corrosion resistance under high temperatures [28]. Nevertheless, these properties involve high cutting forces during machining, low material removal rates, adhesions, and other issues, which enhance premature tool wear [28–33]. In the light of these concerns, selecting this material for experimental case of study implies aggressive machining conditions and becomes suitable in order to test SAM behavior and establish a comparison with conventional milling process.

Regarding tools used during the tests, three types of tools were chosen. In the case of roughing by milling, four teeth carbide tool coated with AlTiN of 16 mm of diameter and 40 mm of cutting length was used. On the other hand, for the finishing operations the tool diameter used was of 6 mm with six teeth, 26 mm of cutting length and coated with TiN/TiAlN. In the case of the first tool, AlTiN coating was chosen because presents higher surface hardness than TiAlN coating and the high presence of aluminum offers better resistance to oxidation in comparison with other coatings [34]. However, the finishing mill was chosen with TiN/TiAlN multi-layer coating with the aim of obtaining a balance between surface roughness and cutting temperature resistance [34]. Nevertheless, it must be taken into account that recently other PVD coatings based on nc-AlCrN/a-Si_3N_4, AlTiCrN with a nanocomposite top layer, TiAlCrN or AlTiCrSiYN/AlTiCrN with 55% of Al in the Si + Y layers were successfully tested for nickel based alloys machining [35–38].

In the case of SAM, the same tool was used in both operations; a PCBN grinding tool of 16 mm of diameter and 20 mm of cutting edge was used. On the other hand, concerning cutting conditions, in order to allow for using SAM technology in this type of machining centers, they were adapted to the spindle capacities. Finally, the cutting fluid chosen to be able to use the grinding tool was a synthetic

emulsion with a concentration of 20%. Tools characteristics, cutting conditions, and operation times are summarized in Table 2.

Table 2. Tools and cutting conditions.

OPERATION	ROUGHING	ROUGHING	FINISHING	FINISHING
	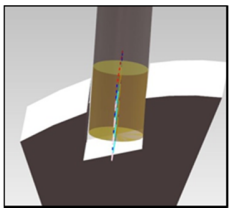	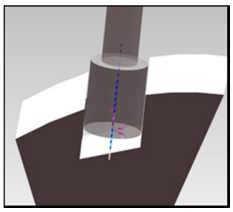	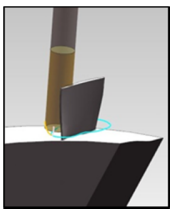	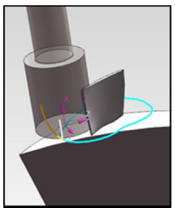
STRATEGY	Milling	Flank SAM	Flank Milling	Flank SAM
				
Cutting Conditions				
F	0.03 mm/tooth	45 mm/min	0.03 mm/tooth	500 mm/min
V_c	20 m/min	900 m/min	40 m/min	900 m/min
a_p	5 mm	20 mm	20 mm	20 mm
a_e	16 mm	16 mm	0.2 mm	0.2 mm
OPER. TIME	3 min 38 s	1 min 43 s	16 s	14 s

In relation to machining strategies, in the case of roughing with milling tools several passes were used to avoid tool break failure. However, with SAM technology it is possible to perform this operation in one only pass/step. On the other hand, in order to carry out finishing strategies, a mathematical algorithm developed in 2016 by Pengbo Bo et al. [39] was used. The use of this algorithm is needed to obtain the surface dimensional requirements in this type of parts where it not allowed any section break/jump between different tool paths along blade surface. These applications occur frequently and this algorithm offers a full solution to perform the machining operations just with one tool path.

This algorithm focuses on approximation of free form surfaces by envelopes of motions of surfaces of revolution (milling tools). This algorithm is perfectly suited for flank milling purposes. However, their approach optimized both the shape of the milling and its trajectory. In this set up, the shape of the (virtual) milling tool was fixed according to the existing (physical) counterpart. The equations that control this algorithm are shown in Equations (1)–(5). In particular, taking "a" and "b" as the two boundary curves and "d" as the unknown distance, Equation (1) represents the whole objective function to obtain this approximation where $\mu_1 = 1$, $\mu_2 = \mu_4 = 0.1$, and $\mu_3 = 0.001$; Equations (2) and (4) correspond to the two components of the objective function that represent the point-surface proximity. Equation (5) controls the rigidity and Equation (3) is the fairness of the two boundary curves to achieve a fair motion.

$$F_{motion}(a,b,d) = \mu_1 F_{plane}(a,b,d) + \mu_2 F_{fair}(a,b) + \mu_3 F_{point}(a,b,d) + \mu_4 F_{rigid}(a,b) \; where, \quad (1)$$

$$F_{plane}(a,b,d) = \frac{1}{mn} \sum_{j=1}^{n} \sum_{i=1}^{m} \left((p_{ij} - p_{ij}^{\perp}, n_{ij}) - d_j \right)^2 \quad (2)$$

$$F_{fair}(a,b) = \frac{1}{m}\sum_{i=2}^{m-1}(a(t_{i-1}) - 2a(t_i) + a(t_{i+1}))^2 + \frac{1}{m}\sum_{i=2}^{m-1}(b(t_{i-1}) - 2b(t_i) + b(t_{i+1}))^2 \quad (3)$$

$$F_{point}(a,b,d) = \frac{1}{mn}\sum_{j=1}^{n}\sum_{i=1}^{m} \parallel p_{ij} - \left(p_{ij}^{\perp}, d_{ij}n_{ij}\right) \parallel^2 \quad (4)$$

$$F_{rigid}(a,b) = \langle a(t_i) - b(t_i), a(t_i) - b(t_i)\rangle - L^2 = 0 \quad (5)$$

In this way, the full length of tool cutting edge is constantly in contact with the non-ruled surface designed and layers are confined to a single one if tool dimension covers all of the surface height. The accuracy of the process is controlled by the error of the objective function (see Equation (1)). Therefore, to take this into account, the surface height used for these tests was 20 mm, that is, the same height dimension of the cutting tool edges.

Finally, after machining tests were conducted, in order to validate SAM technique from an industrial point of view, the blades obtained were scanned with an ATOS GOM and compared with the Computer-aided design (CAD) model. This equipment is based on the triangulation effect with two cameras with a resolution of 17 μm and an accuracy of 35 μm. Afterwards, besides three-dimensional (3D) surface topography of the walls were obtained using a Leica confocal microscope with a resolution of 0.1 nm.

3. Results and Discussion

Each blade was made five times with both techniques in order to validate the results obtained, and the test finishing criteria was taken the finalization of each blade. In Figure 4, the IBR blades machined are shown during roughing and finishing operations with milling and SAM operations. In this this section, the analysis of different results obtained during the experimental tests are set out. In particular, cutting forces and surface roughness are compared between both operations. Afterwards, based on these analyzed results, a scanned IBR blade obtained by SAM is compared to CAD model. The aim of analyzing these parameters is to demonstrate that SAM process is not only a process in which manufacturing time is reduced, but also is technologically a suitable option to be used in the industry because it improves the current milling process.

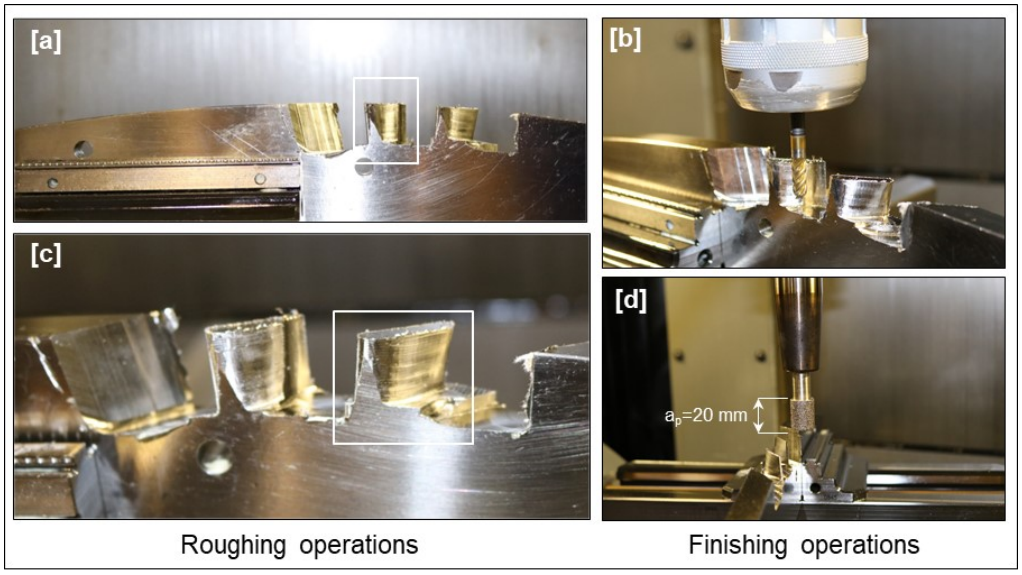

Figure 4. Blades manufacturing process. (**a**) Roughing-Milling; (**b**) Finishing-Milling; (**c**) Roughing-Flank SAM; and, (**d**) Finishing-SAM.

3.1. Cutting Forces

As it was exposed above, forces were registered during IBR blade machining through roughing and finishing operations with milling and SAM techniques. Figure 5 shows total average and maximum total force modulus obtained during the machining processes, as well as estimated errors, which are between ≈2% and ≈7%. Due to the fact that obtained values are below 10%, they are considered admissible [40].

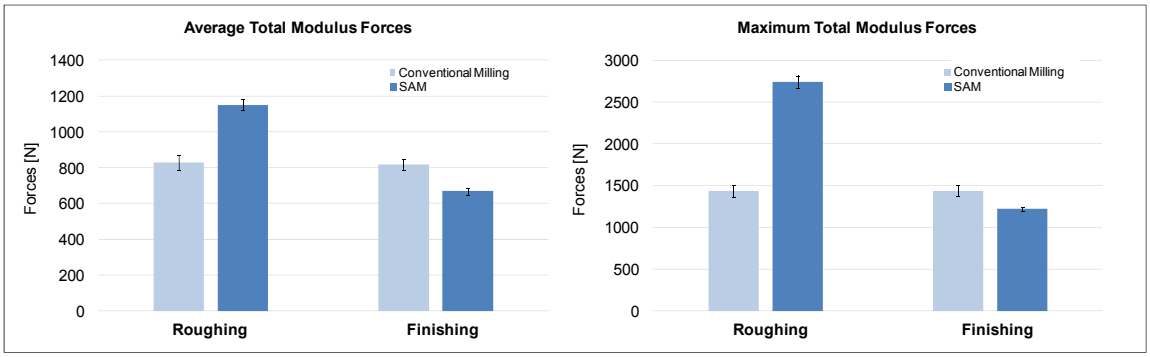

Figure 5. Average and maximum force modulus obtained during blades manufacturing.

As it can be appreciated on the plot, most significant differences between these techniques are recorded during roughing process. It is due to the fact that cutting conditions are more aggressive under these circumstances. SAM medium values overpass 1100 N with a maximum peak over 2500 N. This implies an increase ≈40% and ≈100%, respectively, against traditional milling. This behavior is a result of using one tool pass for Flank SAM when compared to conventional milling with several tool passes; what can be translated into higher material removal rates during SAM and higher forces, but at the same time, a decrease of machining time. In particular, the material removal rate achieved with SAM was 240 mm^3/s what supposes an increase of ≈375% in comparison with conventional milling. These MRR values were calculated in the CAM stage taking into account the material to remove and tool feed as the volume to remove in the operation time. In the non-distant future, it could be calculated by the integral blade rotor weight reduction divided by production time. Nevertheless, finishing process the difference between the two techniques was inverted, obtaining lower force values with SAM than with milling. Concretely, this process presents medium forces around 600 N with a peak of 1200 N. Thus, in comparison with conventional milling, forces are reduced 20% and 15%, respectively.

3.2. Surface Roughness

Regarding surface roughness, the topography and data obtained with the confocal microscope are shown in Figure 6.

Topography in both cases shows a typical surface milling and grinding pattern perfectly generated. This implies stable and controllable cutting process in both cases. However, the differences between both of the technologies are caused by the values obtained in the surface roughness. In the case of milling, the blade surface presents an average roughness (R_a) of 4.85 µm. This value is drastically reduced when SAM technique is used. In this case, the value obtained is 2.66 µm, that is, ≈45% less average roughness in comparison with the milling operation. This behavior is preserved in the mean values of five consecutive maximum heights between peak-valley (R_z). In particular, the values obtained were 49.79 µm and 36.03 µm in the case of milling and SAM machining, respectively. This represents a reduction of ≈28% when SAM is used as machining technology.

Therefore, combining the results obtained regarding cutting forces and surface roughness, SAM technology is suitable for being used to machine IBR blades. With this technology, not only machining times are improved, but also smaller cutting forces during finishing process and better surface

roughness values are obtained. However, another parameter that has to be taken into account is the strict accuracy needed to satisfy the requirements in this type of aeronautical components.

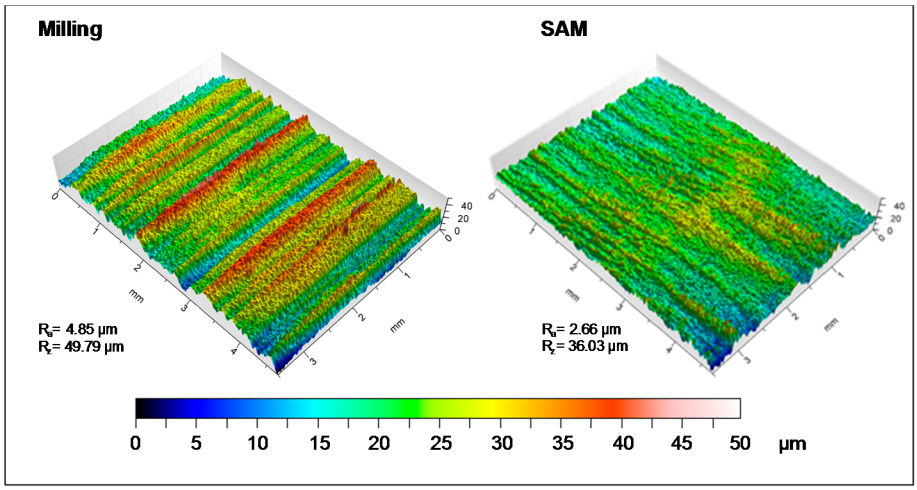

Figure 6. Surface roughness in both processes.

3.3. Dimensional Deviation

In Figure 7 results obtained of comparing the IBR blade manufactured by SAM technology with the CAD model are shown.

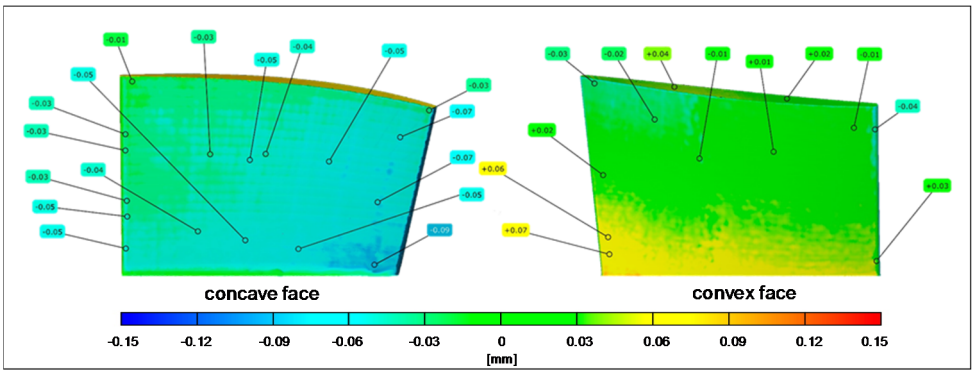

Figure 7. Deviation from nominal geometry.

The results registered present tiny differences, in terms of approximation quality, between the IBR blade obtained by SAM and the CAD model. It should be noted that the tolerances in this type of turbomachinery components need values below 50 µm [41]. In this case, deviations that are obtained are below this value. Nevertheless, overcut is shown in a small area located near the corner. This behavior was found due to the fact that it consists of a non-developable surface, which has to be dealt with a free-form tool to adequate the flank to the defined surface [42]. Thus, the process presented is able to satisfy the requirements in this type of turbomachinery components.

Therefore, results obtained in these experiment show, from a technical point of view related with cutting forces, surface roughness, and dimensional accuracy, which SAM technology does not present a limitation for being used with conventional machines (similar to the one used for this case); as long as cutting conditions were adequately adapted to spindle rotary capacity.

4. Conclusions

In this work, Inconel 718 IBR blades were manufactured with the main objective of comparing milling and SAM techniques in conventional machining centers using oil emulsions instead of mineral cutting oils, reducing its use in ≈80%. For this, both techniques were compared from a technical point of view. In particular, cutting forces, surface roughness and dimensional accuracy were analyzed. The main conclusions obtained are listed below:

- Flank SAM technique applied to roughing operations presented higher material removal rates when compared with conventional milling process, reaching 240 mm^3/s. This means that the process has been optimized through manufacturing time reduction.
- Conversely, this increase of material removal rates is governed by the increase of cutting forces during SAM roughing in a ≈40% and ≈100% for medium and maximum force values, respectively. Nonetheless, in respect to finishing tasks, where material removal rates are similar for both techniques, SAM showed lower cutting forces. In particular, the values are reduced ≈20% and ≈15% for medium and maximum force values, respectively.
- Regarding surface roughness, the topography obtained with both techniques presents a regular pattern that is associated to each technology. However, the surface roughness values present high differences between them. Specifically, the use of SAM technique implies a reduction of ≈45% and ≈28% in R_a and R_z, respectively.
- Concerning dimensional accuracy, the use of SAM generates deviations below the current aeronautical requirements in this type of components.

Therefore, the use of SAM as machining technology implies better results than conventional milling obtaining a suitable, controllable and predictable process to manufacture aeronautical critical components in heat-resistant super alloys, such as Inconel 718, IBR blades presented in this work. Moreover, with this work, the two main restrictions for using SAM as machining process in conventional machining centers with oil emulsions has been avoided.

Acknowledgments: This work is based on TURBO project (DPI2013-46164-C2-1-R) of the Spanish Ministry of Economy and Competitiveness. Also, the authors wish to acknowledge the financial support received from HAZITEK program, from the Department of Economic Development and Infrastructures of the Basque Government and from FEDER founds, related to the project with acronym HEMATEX. Besides, the authors would like to thanks as well to BCAM for its collaboration. Finally, thanks are also addressed to Spanish Project MINECO DPI2016-74845-R and RTC-2014-1861-4.

Author Contributions: Haizea González and Octavio Pereira designed and performed the experiments. On the other hand, Haizea González and Amaia Calleja wrote the paper. Besides, Amaia Calleja analyzed the data related with cutting forces and Naiara Ortega analyzed the data related with surface roughness and dimension accuracy. Michael Barton contributed adapting the mathematical model to the used cutting strategies. Finally, Luis Norberto López de Lacalle contributed with the resources (machine, tools, material . . .) and supervised all the work carried out in this research.

Conflicts of Interest: The authors declare no conflict of interest. The founding sponsors had no role in the design of the study; in the collection, analyses, or interpretation of data; in the writing of the manuscript, and in the decision to publish the results.

References

1. Asociación Española de Tecnologías de Defensa, Aeronáutica y Espacio. Available online: https://www.tedae.org/uploads/attachments/1461082017_retos-del-sector-aeronutico-en-espaa-gua-estratgica-2015-2025-pdf.pdf (accessed on 30 August 2017).
2. Mateo, A. On the feasibility of BLISK produced by linear friction welding. *Revista Metalurgia* **2014**. [CrossRef]
3. Moussaoui, K.; Mouseigne, M.; Senatore, J.; Chieragatti, R.; Lamesle, P. Influence of milling on the fatigue lifetime of a Ti6Al4V titanium alloy. *Metals* **2015**, *5*, 1148–1162. [CrossRef]
4. Klocke, F.; Zeis, M.; Klink, A.; Veselovac, D. Technological and economical comparison of roughing strategies via milling, sinking-EDM, wire-EDM and ECM for titanium- and nickel-based blisks. *CIRP J. Manuf. Sci. Technol.* **2013**, *6*, 198–203. [CrossRef]

5. Pereira, O.; Rodríguez, A.; Barreiro, J.; Fernández-Abia, A.I.; López de Lacalle, L.N. Nozzle design of combined use of MQL and cryogenic gas in machining. *Int. J. Precis. Eng. Manuf. Green Technol.* **2017**, *4*, 87–95. [CrossRef]
6. Klocke, F.; Krämer, K.; Sangermann, H.; Lung, D. Thermo-mechanical tool load during high performance cutting of hard-to-cut materials. *Procedia Fifth Conf. High Perform. Cut.* **2012**, *1*, 295–300. [CrossRef]
7. Thakur, D.G.; Ramamoorthy, B.; Vijayaraghavan, L. Study on the machinability characteristics of superalloy Inconel 718 during high speed turning. *Mater. Des.* **2009**, *30*, 1718–1725. [CrossRef]
8. Modern Machine Shop. Available online: https://www.mmsonline.com/articles/wire-edm-for-jet-engine-fir-trees (accessed on 24 August 2017).
9. Torres, A.; Arbizu, I.; Pérez, C. Analytical modelling of energy density and optimization of the EDM machining parameters of Inconel 600. *Metals* **2017**, *7*, 166. [CrossRef]
10. Sánchez, J.A.; López de Lacalle, L.N.; Lamikiz, A.; Bravo, U. Dimensional accuracy optimisation of multi-stage planetary EDM. *Int. J. Mach. Tools Manuf.* **2002**, *42*, 1643–1648. [CrossRef]
11. Wang, J.; Guo, Y.B.; Fu, C.; Jia, Z. Surface integrity of alumina machines by electrochemical discharge assisted diamond wire sawing. *J. Manuf. Process.* **2018**, *31*, 96–102. [CrossRef]
12. Włodzimierz, W.; Jacek, T. Modern technology of the turbine blades removal machining. In Proceedings of the 8 International Conference Advanced Manufacturing Operations, Kranevo, Bulgary, 18–20 June 2008.
13. Petrilli, R. Super abrasive machining for PM. *Met. Powder Rep.* **2012**, *67*, 38–41. [CrossRef]
14. Erickson, R.E. Method of Machining between Contoured Surfaces with Cup Shaped Tool. U.S. Patent US2011/0189924 A1, 4 August 2011.
15. Erickson, R.E.; Faughnan, P.R., Jr. Method of Machining Integral Bladed Rotors for a Gas Turbine Engine. U.S. Patent 7967659 B2, 28 June 2011.
16. Curtis, D.T.; Soo, S.L.; Aspinwall, D.K.; Sage, C. Electrochemical superabrasive machining of a nickel-based aeroengine alloy using mounted grinding points. *CIRP Ann. Manuf. Technol.* **2009**, *58*, 173–176. [CrossRef]
17. Aspinwall, D.K.; Soo, S.L.; Curtis, D.T.; Mantle, A.L. Profiled superabrasive grinding wheels for the machining of a nickel based superalloy. *CIRP Ann. Manuf. Technol.* **2007**, *56*, 335–338. [CrossRef]
18. Guo, C.; Ranganath, S.; McIntosh, D.; Elfizy, A. Virtual high performance grinding with CBN wheels. *CIRP Ann. Manuf. Technol.* **2008**, *57*, 325–328. [CrossRef]
19. Radical Departures. Available online: https://www.radical-departures.net/articles/flexible-grinding-no-grinder-required/ (accessed on 14 August 2017).
20. Sinha, M.K.; Madarkar, R.; Ghosh, S.; Vao, P.V. Application of eco-friendly nanofluids during grinding of Inconel 718 through small quantity lubrication. *J. Clean. Prod.* **2017**, *141*, 1359–1375. [CrossRef]
21. Iturbe, A.; Hormaetxe, E.; Garay, A.; Arrazola, P.J. Surface integrity analysis when machining Inconel 718 with conventional cryogenic cooling. *Procedia CIRP* **2016**, *45*, 67–70. [CrossRef]
22. Caggiano, A.; Teti, R. CBN grinding performance improvement in aircraft engine components manufacture. *Procedia CIRP* **2009**, *9*, 109–114. [CrossRef]
23. López de Lacalle, L.N.; Lamikiz, A.; Sánchez, J.A.; Cabens, I. Cutting conditions and tool optimization in the high-speed milling of aluminium alloys. *Proc. Inst. Mech. Eng.* **2001**, *215*, 1257–1269. [CrossRef]
24. Suárez, A.; López de Lacalle, L.N.; Polvorosa, R.; Veiga, F.; Wretland, A. Effects of high-pressure cooling on the wear patterns on turning inserts usedon alloy IN718. *Mater. Manuf. Process.* **2017**, *32*, 678–686. [CrossRef]
25. Pottlacher, G.; Hosaeus, H.; Kaschnitz, E.; Seifter, A. Thermophysical properties of solid and liquid Inconel 718 Alloy. *Scand. J. Metall.* **2002**, *31*, 161–168. [CrossRef]
26. Pereira, O.; Urbikain, G.; Rodríguez, A.; Fernández-Valdivielso, A.; Calleja, A.; Ayesta, I.; López de Lacalle, L.N. Internal Cryolubrication approach for Inconel 718 milling. *Procedia Manuf.* **2017**, *13*, 89–93. [CrossRef]
27. Kitagawa, T.; Kubo, A.; Maekawa, K. Temperature and wear of cutting in high-speed machining of Inconel 718 and Ti-6Al-6V-2Sn. *Wear* **1997**, *202*, 142–148. [CrossRef]
28. Razak, N.; Chen, Z.; Pasang, T. Effects of increasing feed rate on tool deterioration and cutting force during end milling of 718plus superalloy using cemented tungsten carbide tool. *Metals* **2017**, *7*, 441. [CrossRef]
29. Mohammed, N.; Makich, H. On the Physics of Machining Titanium Alloys: Interactions between Cutting Parameters, Microstructure and Tool Wear. *Metals* **2014**, *4*, 335–358. [CrossRef]
30. Bhatt, A.; Attia, H.; Vargas, R.; Thomson, V. Wear mechanisms of WC coated and uncoated tools in finish turning of Inconel 718. *Tribol. Int.* **2010**, *43*, 1113–1121. [CrossRef]
31. Hosokawa, A.; Ueda, T.; Onishi, R.; Tanaka, R.; Furumoto, T. Turning of difficult-to-machine materials with actively driven rotary tool. *CIRP Ann. Manuf. Technol.* **2010**, *59*, 89–92. [CrossRef]

32. Costes, J.P.; Guillet, Y.; Poulachon, G.; Dessoly, M. Tool-life and wear mechanisms of CBN tools in machining of Inconel 718. *Int. J. Mach. Tools Manuf.* **2007**, *47*, 1081–1087. [CrossRef]
33. Lamikiz, A.; López de Lacalle, L.N.; Sánchez, J.A.; Bravo, U. Calculation of the specific cutting coefficients and geometrical aspects in sculptured surface machining. *J. Mach. Sci. Technol.* **2005**, *9*, 411–436. [CrossRef]
34. Fernández de Larrinoa, J. Optimización de procesos de recubrimiento para herramientas de corte. In *Tecnologías de Recubrimiento, Métodos de Caracterización y Optimización de las Propiedades*; University of the Basque Country: Bilbao, Spain, 2015.
35. Barthelmä, F.; Frank, H.; Schiffler, M.; Bartsch, A. Hard coatings to improve the machining of nickel based materials. *Procedia CIRP* **2016**, *46*, 294–298. [CrossRef]
36. Beake, B.D.; Fox-Rabinovich. Progress in high temperature nanomechanical testing of coatings for optimising their performance in high speed machining. *Surface Coat. Technol.* **2014**, *255*, 102–111. [CrossRef]
37. Uhlmann, E.; Oyanedel, J.A.; Gerstenberger, R.; Frank, H. nc-AlTiN/a-Si3N4 and nc-AlCrN/a-Si3N4 nanocomposite coatings as protection layer for PCBN tools in hard machining. *Surface Coat. Technol.* **2013**, *237*, 142–148. [CrossRef]
38. Fox-Rabinovich, G.S.; Kvalev, A.I.; Aguirre, M.H.; Beake, B.D.; Yamamoto, K.; Veldhuis, S.C.; Endrino, J.L.; Wainstein, D.L.; Rashkovskiy, A.Y. Design and performance of AlTiN and TiAlCrN PVD coatings for machining of hard to cut materials. *Surface Coat. Technol.* **2009**, *204*, 489–496. [CrossRef]
39. Bo, P.; Barton, M.; Plakhotnik, D.; Pottmann, H. Towards efficient 5-axis flank CNC machining of free-form surfaces via fitting envelopes of surfaces of revolution. *CAD Comput. Aided Des.* **2016**, *79*, 1–11. [CrossRef]
40. Tabernero, I.; Lamikiz, A.; Martínez, S.; Ukar, E.; López de Lacalle, L.N. Modelling of energy attenuation due to powder flow-laser beam interaction during laser cladding process. *J. Mater. Process.* **2012**, *212*, 516–522. [CrossRef]
41. Klocke, F.; Schmitt, R.; Zeis, M.; Heidemanns, L.; Kerkhoff, J.; Heinen, D.; Klink, A. Technological and economical assessment of alternative process chains for blisk manufacture. *Procedia CIRP* **2015**, *35*, 67–72. [CrossRef]
42. Wu, C.Y. Arbitrary surface flank milling & flanksam in the design and manufacturing of jet engine fan and compressor airfoils. In Proceedings of the ASME Turbo Expo 2012 GT 2012, Copenhagen, Denmark, 11–15 June 2012.